Afferent Encoding of Central Oscillations in the Monkey Arm

Stuart N. Baker, Matthew Chiu and Eberhard E. Fetz

J Neurophysiol 95:3904-3910, 2006. doi:10.1152/jn.01106.2005

J Neurophysiol 95: 3904–3910, 2006;
doi:10.1152/jn.01106.2005.

Afferent Encoding of Central Oscillations in the Monkey Arm

Stuart N. Baker,[1] Matthew Chiu,[1] and Eberhard E. Fetz[2]

[1]*University of Newcastle upon Tyne, Sir James Spence Institute, Newcastle upon Tyne, United Kingdom; and* [2]*Department of Physiology and Biophysics and Washington National Primate Research Center, University of Washington, Seattle, Washington*

Submitted 19 October 2005; accepted in final form 22 January 2006

Baker, Stuart N., Matthew Chiu, and Eberhard E. Fetz. Afferent encoding of central oscillations in the monkey arm. *J Neurophysiol* 95: 3904–3910, 2006; doi:10.1152/jn.01106.2005. We have investigated whether peripheral afferent fibers could encode the central oscillations that are commonly seen in the primate motor system. We analyzed 52 single afferent recordings from the C8/T1 dorsal root ganglia of two monkeys performing an isometric wrist flexion–extension task. Coherence and directed coherence were calculated between the afferent spikes and forearm EMG. Seven of 52 cells were identified as Group Ia afferents by the production of narrow postspike facilitation in spike-triggered averages of rectified EMG. These identified afferents showed significant coherence, and directed coherence, with EMG over a wide frequency range. By contrast, coherence was weak for a population that showed little directional preference for flexion or extension movements during task performance, and probably contained mainly cutaneous afferents. Oscillations are known to appear in muscle activity; their presence in afferent firing as well implies that central oscillations pass around a peripheral feedback loop and may be involved in sensorimotor integration.

INTRODUCTION

Cells in the primate motor cortex are capable of transiently synchronizing their discharge to local oscillations in the 20- to 30-Hz range (Baker et al. 1997; Murthy and Fetz 1992). This state appears during rest or steady contraction, but is often abolished by movement (Baker et al. 1997; Murthy and Fetz 1996). Despite much interest, there is as yet no agreement on what function such periodic activity might perform.

Motor cortical oscillations are coherent with those in contralateral electromyograms (EMGs) (Baker et al. 1997; Conway et al. 1995; Murthy and Fetz 1992, 1996). Riddle and Baker (2005) recently provided indirect evidence that this corticomuscular coherence may be mediated by both ascending and descending pathways. They predicted that afferent fibers should also fire in partial synchrony with oscillations in the cortex and muscle. If true, this would open up a significant new range of possibilities for the function of this network state because it would implicate synchronous oscillations in sensorimotor processing, rather than limiting them to a purely "motor" role (MacKay 1997). In this study, we measured the extent to which afferents encode the oscillations seen in EMG, using recordings made directly from the dorsal root ganglia (DRG) in awake behaving monkeys. For those cells most likely to be muscle spindle primary afferents, we find robust coherence, supporting the hypothesis that cortical oscillations are indeed passing around a peripheral feedback loop.

Address for reprint requests and other correspondence: S. Baker, University of Newcastle upon Tyne, Sir James Spence Institute, Royal Victoria Infirmary, Queen Victoria Road, Newcastle upon Tyne, NE1 4LP, UK (E-mail: stuart.baker@ncl.ac.uk).

METHODS

The data set analyzed herein was the subject of a previous report (Flament et al. 1992), which should be consulted for full details of the experimental methods and additional results. Briefly, two *Macaca mulatta* monkeys were trained to perform an isometric wrist flexion–extension task for applesauce reward, and were then implanted with a headpiece, to allow atraumatic head fixation, and a recording chamber placed over the cervical spinal cord to allow access to the C8/T1 DRG. Single units were recorded from the DRG using tungsten microelectrodes while the animal performed the task. The EMG was simultaneously recorded from ≤11 forearm muscles using differential recordings from pairs of implanted wires. In some cases, recordings from up to three electrode pairs were made from the same muscle; such redundant records were averaged together before processing for coherence analysis. All signals were stored on FM or videotape, and subsequently digitized (5,952-Hz sampling rate for EMG, 11,905-Hz rate for single units) using a 1401 laboratory interface (CED, Cambridge, UK). The waveform from the DRG recording was discriminated to yield the occurrence times of single-unit spikes using custom-written cluster-cutting software (GetSpike, S. N. Baker). All records were visually inspected to ensure the accuracy of discrimination. Units with inconsistent spike wave shapes, or with interspike intervals <1 ms, were not used in subsequent analysis.

To detect functional coupling in the frequency domain, coherence and directed coherence were calculated. EMG recordings were rectified, low-pass filtered, and down-sampled to 100-Hz sampling rate. Single-unit spike trains were converted to a waveform by binning spikes in 10-ms intervals. For coherence analysis, the continuous recordings were divided into 1-s-long nonoverlapping sections. Denoting the Fourier transform of the *i*th section of the unit and EMG as $X_i(f)$ and $Y_i(f)$, respectively, the coherence is given by

$$\mathrm{Coh}(f) = \frac{\left|\sum_{i=1}^{L} X_i^*(f) Y_i(f)\right|^2}{\sum_{i=1}^{L} X_i(f) X_i^*(f) \sum_{i=1}^{L} Y_i(f) Y_i^*(f)} \quad (1)$$

where L is the number of data sections available and * denotes complex conjugate.

The coherence phase was determined by

$$\theta(f) = \arg\left[\sum_{i=1}^{L} X_i^*(f) Y_i(f)\right] \quad (2)$$

Coherence is a measure of correlation in the frequency domain. Significant coherence can be generated by numerous patterns of connectivity. By contrast, *directed coherence* measures the extent to which one signal can be predicted by the past history of another (Kaminski and Blinowska 1991). In this sense, directed coherence can

The costs of publication of this article were defrayed in part by the payment of page charges. The article must therefore be hereby marked "*advertisement*" in accordance with 18 U.S.C. Section 1734 solely to indicate this fact.

be interpreted as a measure of causality. The first stage of estimating directed coherence is to fit an autoregressive (AR) model to the observed signals. Using notation similar to Kaminski et al. (2001), let the vector $X(t) = [Unit(t), EMG(t)]^T$ be the activity of unit and EMG at time t. The AR model is then

$$\mathbf{X}(t) = \sum_{i=1}^{p} \mathbf{A}(i)\mathbf{X}(t-i) + \mathbf{E}(t) \quad (3)$$

where $\mathbf{A}(i)$ is a 2×2 matrix of coefficients describing the causal influence of the signals at lag i on the signals at lag zero and $\mathbf{E}(t)$ is a vector of prediction errors at each time point. Transforming this convolution equation to the frequency domain yields, by the convolution theorem (Arfken and Weber 1995)

$$\mathbf{A}(f)\mathbf{X}(f) = \mathbf{E}(f) \quad (4)$$

which can be rewritten as

$$\mathbf{X}(f) = \mathbf{A}^{-1}(f)\mathbf{E}(f) = \mathbf{H}(f)\mathbf{E}(f) \quad (5)$$

where $\mathbf{H}(f)$ is the transfer function of the system. $|H_{ij}(f)|^2$ gives the directional transfer function, representing the causal influence of signal j on signal i. One great advantage of standard coherence is that it is a normalized measure, varying between 0 and 1. Unfortunately, there is no universally accepted normalization for directional coherence. Several authors choose to present nonnormalized values, although these can be difficult to interpret because they depend on the magnitude of the analyzed signals. Others normalize by the sum of all causal influences on the channel under consideration. Here, we have calculated directed coherence as

$$\text{Dir Coh}_{i \leftarrow j}(f) = |H_{ij}(f)|^2 \frac{S_{jj}(f)}{S_{ii}(f)} \quad (6)$$

where S_{kk} is the power spectrum of signal k. The phase of the directed coherence was found by arg $[H_{ij}(f)]$. S may be calculated from the AR model by

$$\mathbf{S}(f) = \mathbf{H}(f)\mathbf{V}\mathbf{H}(f)^H \quad (7)$$

where $\mathbf{V}$ is the covariance matrix of the error terms $\mathbf{E}$ and the superscript H designates the Hermitian conjugate. Using the definition of directed coherence given in *Eq. 6* has the advantage that the measure does not depend on the scale of the signals. Whereas the nonnormalized directed coherence $|H_{ij}(f)|^2$ is proportional to the power of signal i, and inversely proportional to the power of signal j, such dependencies are removed by *Eq. 6*. The values are thus directly comparable between different recordings. Second, we have found that in simulated data where the only interaction is signal 1 causes signal 2, Dir $\text{Coh}_{2 \leftarrow 1}(f)$ equals Coh (f) to within estimation error. However, more complex situations (e.g., 1 causes 2, and 2 causes 1) can produce divergence between directional coherence and coherence. Unlike standard coherence, directional coherence defined as in *Eq. 6* is not bounded by one.

An advantage of standard coherence analysis is that analytical expressions exist for the distribution of coherence. These can be used to estimate a significance limit S, which coherence will exceed by chance only 5% of the time under the null hypothesis that two signals are independent Gaussian-distributed noise (Brillinger 1975)

$$S = 1 - 0.05^{1/(L-1)} \quad (8)$$

No comparable formula has been developed for directed coherence. However, we verified by numerical simulation that under the null hypothesis the distribution of directed coherence, normalized as *Eq. 6*, is very similar to that for standard coherence. We have therefore used the significance limit calculated using *Eq. 8* for both measures.

To improve the estimate of the afferent synchrony related to common central oscillations, we averaged the coherence estimates, and the directed coherence estimates, obtained between an afferent and multiple EMG recordings. The subset of EMGs used varied for each cell, depending on those available in a given recording session. Only coherence calculated with EMGs that were coactivated with the unit were included in such averages (e.g., for an afferent firing only during flexion, EMGs from extensor muscles were excluded). Following the procedure described in Evans and Baker (2003), the expected distribution of such averages, under the null hypothesis, was determined by convolving together the theoretical distributions of the individual coherence values averaged (Brillinger 1975). The 95th percentile of this distribution was used as the significance level for the averaged coherence. This procedure was preferred over pooled spectral analysis (Halliday et al. 2000), which in some circumstances can overestimate the extent of functional coupling (Baker 2000).

There is much literature on the correct choice of the AR model order p. The choice of p will determine the number of bins in the Fourier-transformed model parameters, and thus the frequency resolution to which directional coherence can be estimated. The choice of model order is thus equivalent to the choice of window length for standard spectral analysis. In this work, we used a model order $p = 100$, providing a frequency resolution for our directed coherence measures of 1 Hz, the same as standard coherence.

The parameters of the AR model were fitted to the data using publicly available routines (ArFit; Schneider and Neumaier 2001). All analysis was carried out in the MATLAB environment (The MathWorks). For both standard coherence analysis and directed coherence, the entire available recording was used for analysis. No attempt was made to separate different phases of the task performance because of the limited duration of data available.

RESULTS

Figure 1*A* illustrates raw data for a single afferent recorded during performance of the behavioral task. The power spectrum of this unit showed two clear peaks, at 20 and 29 Hz (Fig. 1*B*). The illustrated EMG [from the extensor carpi radialis (ECR) muscle] contained power over a wide range of frequencies (Fig. 1*C*), a pattern also seen in the mean power spectrum, averaged over all seven EMGs recorded during this experiment (Fig. 1*D*).

Standard coherence analysis between this unit and the ECR muscle EMG (Fig. 1*E*) revealed high coherence at frequencies <10 Hz; this probably reflects the covariation of the unit's firing rate and the EMG activity produced by the task performance (see Fig. 1*A*). In addition, 20/41 bins from 10 to 50 Hz exceeded the theoretical significance limit, marked by the dashed line. No consistent differences were seen in the results obtained with EMG from different muscles. To obtain a better estimate of whether this unit fired synchronously with EMG oscillations, we therefore averaged the unit-EMG coherence spectra obtained from all seven available EMG recordings (Fig. 1*G*). All of these recordings were from extensor muscles, which were coactivated with the unit. The significance limit for this plot is lower than that for Fig. 1*E*, reflecting the improvement in the coherence estimate by averaging over multiple muscles. In the range 18–50 Hz, 30/33 bins had a mean coherence significantly different from zero.

Figures 1, *H–M* shows the results of directed coherence analysis for this unit, in the same format as that for Fig. 1, *E–G*. In both directions, the mean directed coherence was significantly nonzero over a broad frequency range (Fig. 1, *J* and *M*). However, in this afferent the directed coherence for "unit causing EMG" (unit $\rightarrow$ ECR) was larger than in the opposite direction, and had a clear peak centered around 21 Hz (Fig. 1*J*).

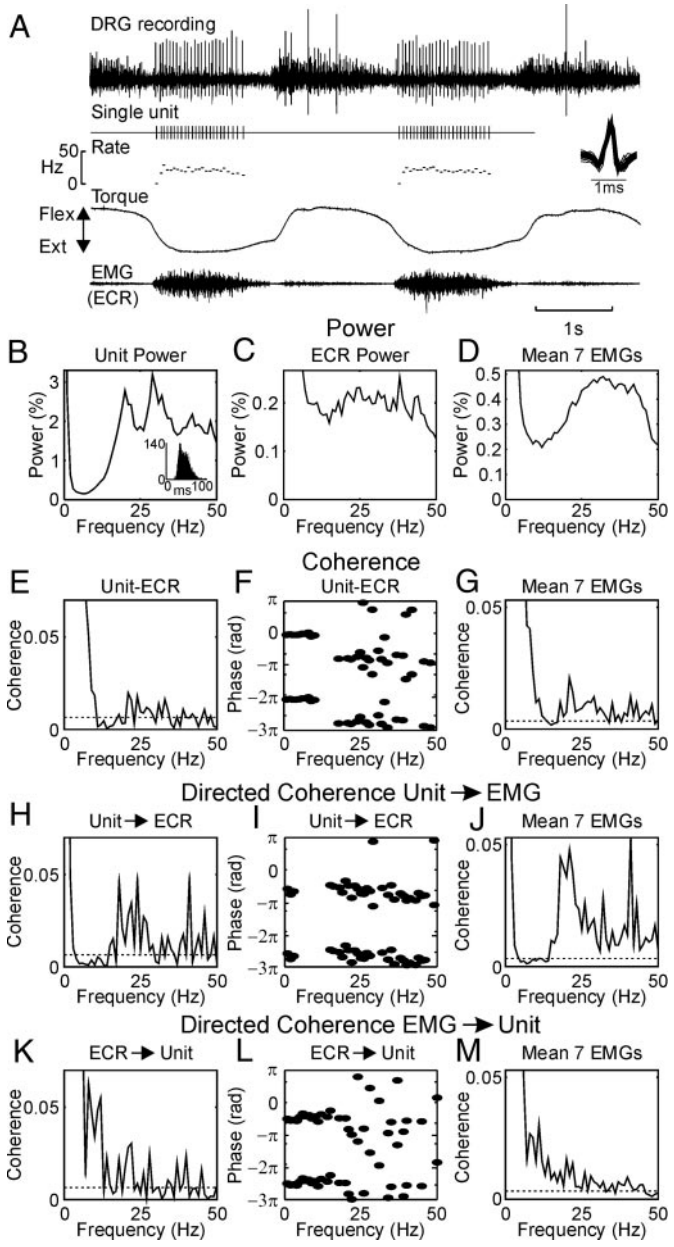

FIG. 1. Example raw data and analysis for a single afferent unit. *A*: raw data traces, showing dorsal root ganglia (DRG) recording and a raster of discriminated single-unit occurrence times. *Inset*: overlain waveforms show the consistent action potential waveform. Also illustrated are instantaneous firing rate, the isometric torque trace, and an electromyogram (EMG) recording from the extensor carpi radialis (ECR) muscle. *B*: power spectrum for this single unit. *Inset*: interspike interval histogram. *C*: power spectrum for the rectified EMG from the ECR muscle. *D*: average power spectrum of all 7 EMGs simultaneously recorded. *E*: coherence between the illustrated unit and the EMG from ECR. *F*: coherence phase. Phase has been plotted for bins only with significant coherence. Each value has been plotted twice, in the range $-\pi$ to π and -3π to $-\pi$, to aid visualization of trends across cycle boundaries. *G*: mean of the coherences between the unit and all 7 EMGs recorded. *H–J*: directed coherence, for the unit causing EMG; and *K–M*, for EMG causing the unit, in the same format as that of *E–G*. Dashed line on coherence plots indicates significance level ($P < 0.05$).

A total of 52 afferent recordings were available for analysis. These ranged in duration from 69 to 1,142 s (mean 374 s). Between 357 and 28,075 spikes were recorded per cell (mean 4,132 spikes); 46 units had >1,000 spikes. Many afferents showed significant coherence and directed coherence with EMG. Of course, these coherence results would be considerably more informative if they could be related to the identity of the afferent. As described by Flament et al. (1992), Group Ia afferents can be identified by spike-triggered averaging (STA) of rectified EMG. The monosynaptic connections these afferents make to motoneurons produce postspike facilitation (PSF). Figure 2*A* shows a STA of EMG from the ECR muscle, for the unit illustrated in Fig. 1. A clear PSF can be seen, which rises above the 95% confidence limits around the baseline (dotted lines). A total of 114 significant PSFs were seen, from 11/52 units.

Unfortunately, the presence of a PSF does not provide definitive proof that the triggering afferent was a Group Ia fiber. As described in Flament et al. (1992), and further investigated by Baker and Lemon (1998), presynaptic synchronization can produce PSF even for a neuron with no monosynaptic connections to motoneurons. Flament et al. (1992) showed by stimulation that the minimal conduction time from DRG to muscle in these recordings was 3.5 ms. PSFs with onset latency earlier than this probably contain a synchrony component. Baker and Lemon (1998) advised measurement of the peak width at half-maximum (PWHM): PSFs generated by synchrony have wider peaks than those arising from monosynaptic input to motoneurons. However, the limit on PWHM that should be used will depend on the parameters of presynaptic synchrony. For motor cortical neurons, for which data on synchrony are available, Baker and Lemon (1998) suggested PSFs with PWHM <7ms could be reliably interpreted as indicating cortico-motoneuronal cells. No such data on afferent synchronization are available, so a theoretically derived limit on PWHM cannot be determined.

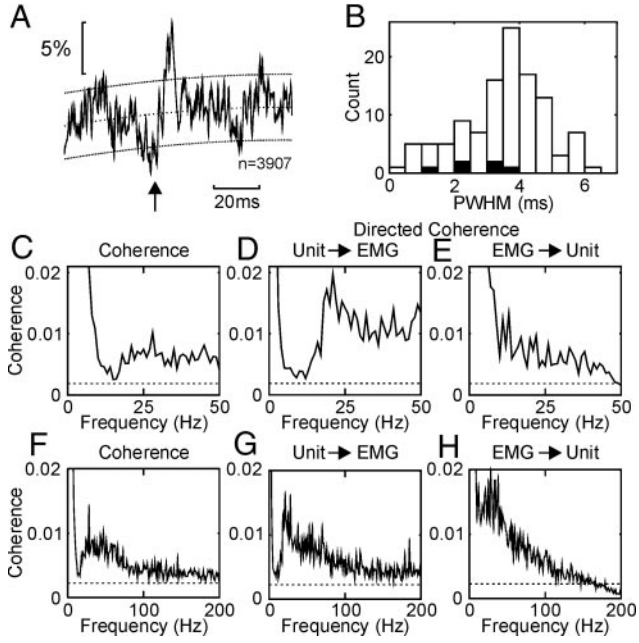

FIG. 2. *A*: spike-triggered average of ECR EMG, with the unit illustrated in Fig. 1 as the trigger. Dashed line shows baseline; dotted lines show estimated 95% confidence limits on the baseline. Arrow marks the time of the spike. *B*: distribution of the peak width at half-maximum (PWHM) of all significant postspike facilitations (PSFs) observed. Black bars indicate PSFs with an onset latency >3.5 ms. *C–E*: EMG-unit coherence and directed coherence averaged across the 7 units with PWHM ≤4 ms. Measures have been averaged across all EMGs recorded with each unit. *F–H*, like *C–E*, but with analysis parameters altered to allow examination of frequencies ≤200 Hz.

Figure 2*B* shows the distribution of PWHM for all 114 significant PSFs that were observed. The six PSFs with onset latency >3.5 ms all had PWHM ≤4 ms (black bars); the PSF shown in Fig. 2*A* is one such unit. We therefore suggest that PWHM ≤4 ms is a reasonable criterion to distinguish PSF produced by Group Ia afferents from that which might be generated solely by synchronization. Seven of 11 units had a narrow PSF in at least one STA and were thus classified as Group Ia in origin. This is a highly conservative criterion: it is likely that some of the other units were Group Ia, but that their PSFs were wider than these stringent criteria because of synchrony effects or dispersion of the motor unit potentials (for discussion of the use of such criteria, see Baker and Lemon 1998; for contributions to width, see Palmer and Fetz 1985).

Figure 2, *C–E* shows the coherence measures, averaged over all EMG recordings available for each unit, and over the seven putative Ia afferents. The standard coherence is significantly nonzero for all bins displayed (Fig. 2*C*), although there is a clear dip around 16 Hz. Oscillations in the beta frequency range in the EMG (see Fig. 1*D*) will therefore be represented in the discharge of these single afferent units. Although the coherence is low (about 0.007), this is within the range observed for corticomuscular coherence in both humans and monkeys (Baker et al. 1997; Kilner et al. 2000). Baker et al. (2003) and Soteropoulos and Baker (2006) argued that such low levels of coherence probably result from nonlinearities of neural spiking, and may nevertheless indicate quite strong levels of functional coupling.

There are multiple possible pathways that could generate the observed coherence between Group Ia afferents and EMG. First these afferents make monosynaptic connections to motoneurons. The directed coherence (Unit → EMG, Fig. 2*D*) was significantly nonzero at all frequencies, with a clear peak around 20 Hz. When the directed coherence phase for this direction was plotted versus frequency, a linear relationship was often observed in the 15- to 50-Hz range (see example in Fig. 1*I*). Such a relationship is indicative of a constant time delay between the two signals. A regression line fitted to this relationship (with phases from all muscles overlain to improve the quality of the fit) had a slope significantly different from zero for five of seven afferents; the mean slope corresponded to a delay of 11.8 ms (range 7–21 ms). This is consistent with the delay expected from monosynaptic connectivity.

Directed coherence in the opposite direction (EMG → Unit) was also significant over a wide frequency range (Fig. 2*E*). This could be produced by two routes. First whenever motor units are active, they will generate both twitch tensions and motor unit action potentials in the EMG. Oscillatory muscle activity can thus produce mechanical tremor. Group Ia afferents are especially sensitive to small-amplitude stretches of the muscle spindle and could detect such tremor (Matthews 1972). This would generate directional coherence in the EMG → unit direction. However, motor unit twitch times for forearm muscles are around 50–100 ms (Riddle and Baker 2005); a mechanical route for the observed directed coherence should therefore generate a considerable delay. Only three of seven units showed a significant linear relationship between the directed coherence phase and frequency. For two of these afferents, the delay implied by the regression slope was 40.6 and 41 ms; for these cells, a mechanical linkage appears likely. However, the remaining afferent had an inferred delay of only 17.6 ms; the other four units showed no evidence for a linear regression slope significantly different from zero.

For these cells, an alternative possibility is the presence of beta innervation of the muscle spindles. In this case, the beta motoneurons would produce motor unit action potentials in the EMG, and also generate twitches in the intrafusal fibers that would directly excite the afferents. The delay from activation of the spindle motor fibers to an increase in Ia afferent firing rate is <10 ms (Bessou et al. 1968). For the four afferents with phase-frequency slopes not significantly different from zero, this route therefore appears more likely than a functional connection by overt movement produced by the extrafusal fibers.

The primary focus of this study is the "beta" range of about 15–35 Hz, at which frequencies oscillations are observed in sensorimotor cortex. However, Fig. 2, *C–E* shows that the coherence between afferents and EMG was not limited to this range. To examine this further, analysis for these seven afferents was repeated with the data downsampled to 400 Hz, rather than the 100 Hz used originally. This permitted examination of the spectral measures for frequencies ≤200 Hz. The majority of coherence and directed coherence was seen at frequencies <100 Hz (Fig. 2, *F–H*), although coherence was still significantly nonzero up to 200 Hz.

It is difficult to assign the remaining afferents to receptor categories with any degree of reliability: receptive field mapping could not routinely be carried out in these animals because of the precarious nature of the recordings. However, one further distinct subclass of afferent did emerge from the firing patterns during task performance. Like the example shown in Fig. 1*A*, most afferents were active predominantly during one phase of the task (flexion or extension). However, a minority spiked almost equally during both types of movement; an example of such a recording is shown in Fig. 3*A*. This cell did not show significant PSF in STAs (Fig. 3*B*).

To quantify the directional specificity of a cell, we computed a directional index

$$D = \frac{\left| \frac{1}{n} \sum_{i=1}^{n} F(t_i) \right|}{\sqrt{\frac{1}{n} \sum_{i=1}^{n} F^2(t_i)}} \quad (9)$$

where the times of the n spikes recorded are t_i and F is the manipulandum torque (positive for flexion, negative for extension). So defined, D will be close to one for afferents that fire only during one task phase, but close to zero for those that spike equally during flexion and extension. Figure 3*C* shows the distribution of the directionality index over all 52 afferents recorded. This appears to be a bimodal distribution; we accordingly denoted the 18 afferents with D <0.4 as "bidirectional units." Although Group Ia afferents may show bidirectional firing (Flament et al. 1992; Schieber and Thach 1985), they usually display a preference for one direction. All seven units identified as Group Ia afferents in this study showed D >0.85 (hatched bins in Fig. 3*C*). The afferents with D <0.4 were by contrast genuinely bidirec-

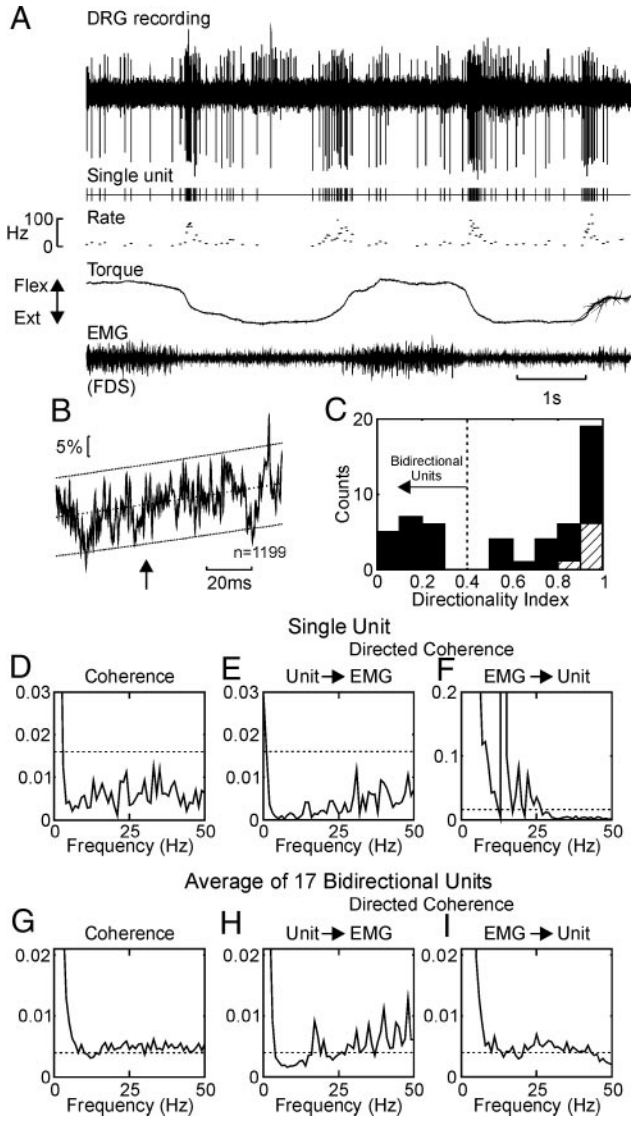

FIG. 3. *A*: example raw data for a single unit that fired in both extension and flexion phases of the task; layout as in Fig. 1*A*. *B*: spike-triggered average of flexor digitorum superficialis (FDS) muscle EMG triggered by this unit, showing lack of significant PSF. *C*: distribution of directionality index ($n = 52$ units). Values <0.4 were assumed to represent bidirectional firing. Hatched bins indicate units classified as Group Ia on the basis of PSF in spike-triggered averages. *D–F*: unit-EMG coherence and directed coherence for a single, anomalous, bidirectional unit, averaged over all 7 recorded EMGs. Notice the different scale in *F*; peak at 14 Hz has been truncated. *G–I*: mean unit-EMG coherence and directed coherence, averaged over the remaining 17 bidirectional units and all recorded EMGs.

tional, and we suggest that most of these afferents are likely to be cutaneous in origin. In only one of these units did STAs show significant PSFs. However, these had an onset latency clearly before the trigger, and PWHM >4 ms, compatible with generation by presynaptic synchronization.

Coherence analysis for these 18 afferents revealed a consistent pattern, except for one anomalous unit whose results are presented in Fig. 3, *D–F*. This afferent had nonsignificant coherence in all bins >2 Hz (Fig. 3*D*), and no significant directed coherence in the unit → EMG direction (Fig. 3*E*). However, directed coherence in the EMG → unit direction showed a peak of 8.5 at 14 Hz (truncated in Fig. 3*F* for clarity of display). Examination of the directed coherence phase showed a significant linear phase–frequency relationship for all muscles, with slopes implying a delay between 19 and 104 ms (mean 80 ms). Such results are consistent with this unit detecting mechanical tremor produced by extrafusal contractions. Several cutaneous receptor classes might be capable of detecting such small fluctuations; the most likely type is the Pacinian corpuscle, which has a threshold as low as 1 μm (Johansson et al. 1982).

Figure 3, *G–I* presents averaged coherence spectra for the remaining 17 bidirectional units. Although both coherence and directed coherence did rise just above the theoretical significance limit, they were weak compared with the measurements from the identified Group Ia afferents in Fig. 2, *C–E*.

DISCUSSION

In this report, we have examined synchronization between single afferent units and EMG in the frequency domain. Descending input to motoneurons from the corticospinal tract is probably responsible for the commonly observed approximately 25-Hz oscillations in muscle activity (Baker et al. 1997; Conway et al. 1995; Farmer et al. 1993). Accordingly, by measuring afferent-EMG coherence, we were effectively assessing the extent to which afferents represented these centrally generated oscillations in their discharge. Those units most likely to be Group Ia muscle spindle afferents showed significant coherence with EMG over a broad frequency range. Using directed coherence, we found that this coherence resulted both from the unit influencing the EMG (probably by monosynaptic connections) and also from the unit entraining with oscillations in the motor output (probably mainly by beta innervation of spindles). By comparison coherence was weak in a different subpopulation of units, most of which were likely cutaneous in origin.

Although several of our coherence and directed coherence spectra showed clear peaks around 20 Hz (Figs. 1, *G* and *J*, and 2*D*), on average putative Group Ia afferents had significant coherence over a broad frequency range (Fig. 2, *F–H*). This indicates that a wide range of oscillatory frequencies, and not just those in the "beta " band, are capable of traversing the afferent feedback loop. However, it was previously demonstrated that an isometric task, as used here, leads to smaller beta-band oscillatory activity than tasks in which the hand is allowed to move (Kilner et al. 2000). It is thus possible that a more distinct peak around 20 Hz would have been seen using a nonisometric task.

A previous study (Wessberg and Vallbo 1995) reported that firing in muscle afferents was phase locked to the 8- to 10-Hz discontinuities in finger acceleration that are a prominent feature of slow finger movements. In this study, we showed coherence between EMG and afferent discharge at higher frequencies, during a rapid step-hold isometric task. In marked contrast to the work of Wessberg and Vallbo (1995), we often observed a pronounced dip in coherence around 10 Hz (e.g., Fig. 2, *C* and *D*). This probably reflects the very different nature of the network activity during slow finger movements and steady contractions: the former are dominated by 8- to 10-Hz peripheral oscillations, whereas in the latter motoneuron

pools are driven by cortical signals around 20 Hz, and input at about 10 Hz appears to be prevented from synchronizing motoneurons (Baker et al. 2003). It was previously suggested that some neural mechanism (as yet unidentified) might act as an active filter, removing 10-Hz descending input to motoneurons (Baker et al. 2003). The small 10-Hz coherence in the present findings implies that such a system, if it exists, is also capable of removing this frequency band from naturally occurring afferent input.

In an additional difference, the previous work by Wessberg and Vallbo (1995) reported that afferents responded to overt mechanical fluctuations. Analysis of directed coherence phase from our recordings suggested that EMG often influenced unit discharge by beta efferent innervation of the spindles, rather than by a mechanical route.

Several previous reports have shown that sensorimotor cortical oscillations modulate with sensory input. Synchronous bursts of afferent input, produced by electrical nerve stimulation, abolish cortical oscillations and corticomuscular coherence (a stimulus-evoked desynchronization); 1–2 s later the oscillations then rebound to a stronger level than before the stimulus (Hansen et al. 2004; Muller et al. 2003; Salenius et al. 1997). By contrast, in a human subject with large-fiber sensory neuropathy, oscillatory synchronization between different muscles was absent (Kilner et al. 2004). In healthy human subjects, corticomuscular coupling was significantly reduced after a digital nerve block inducing cutaneous anesthesia (Fisher et al. 2002). None of these studies can be directly compared with the present finding, which shows that during normal contractions in intact animals, the sustained afferent discharge is coherent with ongoing central oscillations. However, the previous work does suggest that cortical oscillations are intimately involved with sensory processing, a conclusion further supported by our present findings.

Although only a small number of afferents were assigned to the Group Ia class, it is likely that most of the remaining unidirectional afferents were muscle receptors—either spindle primaries or secondaries—or Golgi tendon organs. Many of these unclassified afferents also showed significant coherence with EMG. Our results therefore provide strong evidence that central oscillations do pass around a peripheral feedback loop, as suggested by Riddle and Baker (2005). We speculate that such a system could be used for recalibration of the motor system after a movement. By measuring the response to a known oscillatory output, the brain could make a more detailed assessment of the state of the periphery than would be provided by tonic discharge (MacKay 1997); such an oscillatory probe could function in a manner analogous to radar or sonar mechanisms. Whether or not this speculation proves valid, the finding that peripheral afferents can encode central oscillations should stimulate further experiments and hypotheses to elucidate the function of this mode of activity.

ACKNOWLEDGMENTS

The authors thank Drs. Didier Flament and Pierre Fortier for permission to reanalyze archived data.

GRANTS

This work was supported by a grant from The Wellcome Trust to S. N. Baker, a grant from The Physiological Society to M. Chiu, and National Institutes of Health Grants NS-12542 and RR-0016 to E. E. Fetz.

REFERENCES

Arfken GB and Weber HJ. *Mathematical Methods for Physicists.* San Diego, CA: Academic Press, 1995, p. 863.

Baker SN. "Pooled coherence" can overestimate the significance of coupling in the presence of inter-experiment variability. *J Neurosci Methods* 96: 171–172, 2000.

Baker SN and Lemon RN. A computer simulation study of the production of post-spike facilitation in spike triggered averages of rectified EMG. *J Neurophysiol* 80: 1391–1406, 1998.

Baker SN, Olivier E, and Lemon RN. Task dependent coherent oscillations recorded in monkey motor cortex and hand muscle EMG. *J Physiol* 501: 225–241, 1997.

Baker SN, Pinches EM, and Lemon SN. Synchronisation in monkey motor cortex during a precision grip task. II. Effect of oscillatory activity on corticospinal output. *J Neurophysiol* 89: 1941–1953, 2003.

Bessou P, Laporte Y, and Pages B. Frequencygrams of spindle primary endings elicited by stimulation of static and dynamic fusimotor fibres. *J Physiol* 196: 47–63, 1968.

Brillinger DR. Time series. Data Analysis and Theory. New York: Holt, Rinehart & Winston, 1975.

Conway BA, Halliday DM, Farmer SF, Shahani U, Maas P, Weir AL, and Rosenberg JR. Synchronization between motor cortex and spinal motoneuronal pool during the performance of a maintained motor task in man. *J Physiol* 489: 917–924, 1995.

Evans CMB and Baker SN. Task dependent inter-manual coupling of 10-Hz discontinuities during slow finger movements. *Eur J Neurosci* 18: 453–456, 2003.

Farmer SF, Bremner FD, Halliday DM, Rosenberg JR, and Stephens JA. The frequency content of common synaptic inputs to motoneurones studied during voluntary isometric contraction in man. *J Physiol* 470: 127–155, 1993.

Fisher RJ, Galea MP, Brown P, and Lemon RN. Digital nerve anaesthesia decreases EMG-EMG coherence in a human precision grip task. *Exp Brain Res* 145: 207–214, 2002.

Flament D, Fortier PA, and Fetz EE. Response patterns and post-spike effects of peripheral afferents in dorsal root ganglia of behaving monkeys. *J Neurophysiol* 67: 875–889, 1992.

Halliday DM and Rosenberg JR. On the application, estimation and interpretation of coherence and pooled coherence. *J Neurosci Methods* 100: 173–174, 2000.

Hansen NL and Nielsen JB. The effect of transcranial magnetic stimulation and peripheral nerve stimulation on corticomuscular coherence in humans. *J Physiol* 561: 295–306, 2004.

Johansson RS, Landström U, and Lundström R. Responses of mechanoreceptive afferent units in the glabrous skin of the human hand to sinusoidal skin displacements. *Brain Res* 244: 17–25, 1982.

Kaminski M, Ding M, Truccolo WA, and Bressler SL. Evaluating causal relations in neural systems: granger causality, directed transfer function and statistical assessment of significance. *Biol Cybern* 85: 145–157, 2001.

Kaminski MJ and Blinowska KJ. A new method of the description of the information flow in the brain structures. *Biol Cybern* 65: 203–210, 1991.

Kilner JM, Baker SN, Salenius S, Hari R, and Lemon RN. Human cortical muscle coherence is directly related to specific motor parameters. *Neuroscience* 20: 8838–8845, 2000.

Kilner JM, Fisher RJ, and Lemon RN. Coupling of oscillatory activity between muscles is strikingly reduced in a deafferented subject compared with normal controls. *J Neurophysiol* 92: 790–796, 2004.

MacKay WA. Synchronised neuronal oscillations and their role in motor processes. *Trends Cogn Sci* 1: 176–182, 1997.

Matthews P. *Mammalian Muscle Receptors and Their Central Actions.* London: Arnold, 1972.

Müller GR, Neuper C, Rupp R, Keinrath C, Gerner HJ, and Pfurtscheller G. Event-related beta EEG changes during wrist movements induced by functional electrical stimulation of forearm muscles in man. *Neurosci Lett* 340: 143–147, 2003.

Murthy VN and Fetz EE. Coherent 25- to 35-Hz oscillations in the sensorimotor cortex of awake behaving monkeys. *Proc Natl Acad Sci USA* 89: 5670–5674, 1992.

Murthy VN and Fetz EE. Oscillatory activity in sensorimotor cortex of awake monkeys: synchronization of local field potentials and relation to behavior. *J Neurophysiol* 76: 3949–3967, 1996.

Palmer SS and Fetz EE. Effects of single intracortical microstimuli in motor cortex on activity of identified forearm motor units in behaving monkeys. *J Neurophysiol* 54: 1194–1212, 1985.

Riddle CN and Baker SN. Manipulation of peripheral neural feedback loops alters human corticomuscular coherence. *J Physiol* 566: 625–639, 2005.

Salenius S, Schnitzler A, Salmelin R, Jousmaki V, and Hari R. Modulation of human cortical rolandic rhythms during natural sensorimotor tasks. *Neuroimage* 5: 221–228, 1997.

Schieber MH and Thach WT. Trained slow tracking. II. Bi-directional discharge patterns of cerebellar nuclear, motor cortex, and spindle afferent neurons. *J Neurophysiol* 54: 1228–1270, 1985.

Schneider T and Neumaier A. Algorithm 808: ARfit—a Matlab package for the estimation of parameters and eigenmodes of multivariate autoregressive models. *ACM Trans Math Softw* 27: 58–65, 2001.

Soteropoulos DS and Baker SN. Cortico-cerebellar coherence during a precision grip task in the monkey. *J Neurophysiol* 95: 1194–1206, 2006.

Wessberg J and Vallbos AK. Coding of pulsatile motor output by human muscle afferents during slow finger movements. *J Physiol* 485: 271–282, 1995.